

1 Genomic and phenomic insights from an atlas of 2 genetic effects on DNA methylation

3 Josine L. Min^{1,2*}, Gibran Hemani^{1,2*}, Eilis Hannon³, Koen F. Dekkers⁴, Juan Castillo-Fernandez⁵,
4 René Luijk⁴, Elena Carnero-Montoro^{5,6}, Daniel J. Lawson^{1,2}, Kimberley Burrows^{1,2}, Matthew
5 Suderman^{1,2}, Andrew D. Bretherick⁷, Tom G Richardson^{1,2}, Johanna Klughammer⁸, Valentina
6 Iotchkova⁹, Gemma Sharp^{1,2}, Ahmad Al Khleifat¹⁰, Aleksey Shatunov¹⁰, Alfredo Iacoangeli^{10,11},
7 Wendy L McArdle², Karen M Ho², Ashish Kumar^{12,13,14}, Cilla Söderhäll¹⁵, Carolina Soriano-
8 Tárraga¹⁶, Eva Giralto-Steinhauer¹⁶, Nabila Kazmi^{1,2}, Dan Mason¹⁷, Allan F McRae¹⁸, David L
9 Corcoran¹⁹, Karen Sugden^{19,20}, Silva Kasela²¹, Alexia Cardona^{22,23}, Felix R. Day²², Giovanni
10 Cugliari^{24,25}, Clara Viberti^{24,25}, Simonetta Guarrera^{24,25}, Michael Lerro²⁶, Richa Gupta^{27,28},
11 Sailalitha Bollepalli^{27,28}, Pooja Mandaviya²⁹, Yanni Zeng^{7,30,31}, Toni-Kim Clarke³², Rosie M
12 Walker^{33,34}, Vanessa Schmoll³⁵, Darina Czamara³⁵, Carlos Ruiz-Arenas^{36,37,38}, Faisal I
13 Rezwani³⁹, Riccardo E Marioni^{34,40}, Tian Lin¹⁸, Yvonne Awaloff³⁵, Marine Germain⁴¹, Dylan
14 Aïssi⁴², Ramona Zwamborn⁴³, Kristel van Eijk⁴³, Annelot Dekker⁴³, Jenny van Dongen⁴⁴, Jouke-
15 Jan Hottenga⁴⁴, Gonneke Willemsen⁴⁴, Cheng-Jian Xu⁴⁵, Guillermo Barturen⁶, Francesc Català-
16 Moll⁴⁶, Martin Kerick⁴⁷, Carol Wang⁴⁸, Phillip Melton⁴⁹, Hannah R Elliott^{1,2}, Jean Shin^{50,51}, Manon
17 Bernard⁵⁰, Idil Yet⁵, Melissa Smart⁵², Tyler Gorrie-Stone⁵², Chris Shaw^{10,53}, Ammar Al
18 Chalabi^{10,53,54}, Susan M Ring^{1,2}, Göran Pershagen¹², Erik Melén^{12,55}, Jordi Jiménez-Conde¹⁶,
19 Jaume Roquer¹⁶, Debbie A Lawlor^{1,2}, John Wright¹⁷, Nicholas G Martin⁵⁶, Grant W
20 Montgomery¹⁸, Terrie E Moffitt^{19,20,57,60}, Richie Poulton⁵⁸, Tõnu Esko^{21,59}, Lili Milani²¹, Andres
21 Metspalu²¹, John R. B. Perry²², Ken K. Ong²², Nicholas J Wareham²², Giuseppe Matullo^{24,25},
22 Carlotta Sacerdote^{25,61}, Avshalom Caspi^{19,20,57,60}, Louise Arseneault⁶⁰, France Gagnon²⁶, Miina
23 Ollikainen^{27,28}, Jaakko Kaprio^{27,28}, Janine F Felix^{62,63,64}, Fernando Rivandeiro²⁹, Henning
24 Tiemeier^{65,66}, Marinus H van IJzendoorn^{67,68}, André G Uitterlinden²⁹, Vincent WV Jaddoe^{62,63,66},
25 Chris Haley⁷, Andrew M McIntosh^{32,34}, Kathryn L Evans^{33,34}, Alison Murray⁶⁹, Katri Räikkönen⁷⁰,
26 Jari Lahti⁷⁰, Ellen A Nohr^{71,72}, Thorkild IA Sørensen^{1,2,73,74}, Torben Hansen⁷³, Camilla Schmidt
27 Morgen⁷⁵, Elisabeth B Binder^{35,76}, Susanne Lucae³⁵, Juan Ramon Gonzalez^{36,37,38}, Mariona
28 Bustamante^{36,37,38,77}, Jordi Sunyer^{36,37,38,78}, John W Holloway^{39,79}, Wilfried Karmaus⁸⁰, Hongmei
29 Zhang⁸⁰, Ian J Deary³⁴, Naomi R Wray^{18,81}, John M Starr^{34,82}, Marian Beekman⁴, Diana van
30 Heemst⁸³, P Eline Slagboom⁴, Pierre-Emmanuel Morange⁸⁴, David-Alexandre Trégouët⁴¹, Jan
31 H. Veldink⁴³, Gareth E Davies⁸⁵, Eco JC de Geus⁴⁴, Dorret I Boomsma⁴⁴, Judith M Vonk⁸⁶, Bert
32 Brunekreef^{87,88}, Gerard H. Koppelman⁴⁵, Marta E Alarcón-Riquelme^{6,12}, Rae-Chi Huang⁸⁹, Craig
33 Pennell⁴⁸, Joyce van Meurs²⁹, M. Arfan Ikram⁶³, Alun D Hughes⁹⁰, Therese Tillin⁹⁰, Nish
34 Chaturvedi⁹⁰, Zdenka Pausova⁴⁹, Tomas Paus⁹¹, Timothy D Spector⁵, Meena Kumari⁵², Leonard
35 C Schalkwyk⁵², Peter M Visscher^{18,81}, George Davey Smith^{1,2}, Christoph Bock⁸, Tom R Gaunt^{1,2},
36 Jordana T Bell⁵, Bastiaan T. Heijmans⁴, Jonathan Mill³, Caroline L Relton^{1,2}

37
38 * These authors contributed equally to this research.

39
40 **Corresponding author:** Josine L Min, josine.min@bristol.ac.uk

43 Affiliations

- 44 ¹ MRC Integrative Epidemiology Unit, University of Bristol, Bristol, UK
45 ² Population Health Sciences, Bristol Medical School, University of Bristol, Bristol, UK
46 ³ University of Exeter Medical School, UK
47 ⁴ Molecular Epidemiology, Department of Biomedical Data Sciences, Leiden University Medical
48 Center, Leiden, The Netherlands
49 ⁵ Department of Twin Research and Genetic Epidemiology, King's College London, London, UK
50 ⁶ Pfizer - University of Granada - Andalusian Government Center for Genomics and Oncological
51 Research (GENYO), Spain
52 ⁷ MRC Human Genetic Unit, Institute of Genetics and Molecular Medicine, University of
53 Edinburgh, Edinburgh, UK
54 ⁸ CeMM, Austrian Academy of Sciences, Vienna, Austria
55 ⁹ MRC Weatherall Institute of Molecular Medicine, Oxford, UK
56 ¹⁰ Department of Basic and Clinical Neuroscience, Maurice Wohl Clinical Neuroscience Institute,
57 London, UK
58 ¹¹ Department of Biostatistics and Health Informatics, King's College London, London, UK
59 ¹² Institute of Environmental Medicine, Karolinska Institutet, Stockholm, Solna, Sweden
60 ¹³ Chronic Disease Epidemiology unit, Swiss Tropical and Public Health Institute, Basel,
61 Switzerland
62 ¹⁴ University of Basel, Basel, Switzerland
63 ¹⁵ Department of Women's and Children's Health, Karolinska Institutet, Stockholm, Sweden
64 ¹⁶ Neurology Department, Hospital del Mar - IMIM (Institut Hospital del Mar d'Investigacions
65 Mèdiques), Barcelona, Spain
66 ¹⁷ Bradford Institute for Health Research, Bradford, UK
67 ¹⁸ Institute for Molecular Bioscience, University of Queensland, Australia
68 ¹⁹ Center for Genomic and Computational Biology, Duke University, Durham, NC, USA
69 ²⁰ Department of Psychology and Neuroscience, Duke University, Durham, NC, USA
70 ²¹ Estonian Genome Center, Institute of Genomics, University of Tartu, Estonia
71 ²² MRC Epidemiology Unit, University of Cambridge, School of Clinical Medicine, Institute of
72 Metabolic Science, Cambridge Biomedical Campus, Cambridge CB2 0QQ, United Kingdom
73 ²³ Department of Genetics, University of Cambridge, Downing Street, Cambridge CB2 3EH,
74 United Kingdom
75 ²⁴ Department of Medical Sciences, University of Turin, Turin, Italy
76 ²⁵ Italian Institute for Genomic Medicine (IIGM), Turin, Italy
77 ²⁶ University of Toronto, Toronto, Canada
78 ²⁷ Institute for Molecular Medicine, University of Helsinki, Helsinki, Finland
79 ²⁸ Department of Public Health, Faculty of Medicine, University of Helsinki, Helsinki, Finland
80 ²⁹ Department of Internal Medicine, Erasmus University Medical Center, Rotterdam, The
81 Netherlands
82 ³⁰ Faculty of Forensic Medicine, Zhongshan School of Medicine, Sun Yat-Sen University,
83 Guangzhou, China
84 ³¹ Guangdong Province Key Laboratory of Brain Function and Disease, Zhongshan School of
85 Medicine, Sun Yat-Sen University, Guangzhou, China
86 ³² Division of Psychiatry, Royal Edinburgh Hospital, University of Edinburgh, Edinburgh EH10
87 5HF, UK
88 ³³ Medical Genetics Section, Centre for Genomic and Experimental Medicine, Institute of
89 Genetics and Molecular Medicine, Western General Hospital, University of Edinburgh, Crewe
90 Road, Edinburgh EH4 2XU, UK
91 ³⁴ Centre for Cognitive Ageing and Cognitive Epidemiology, Department of Psychology,
92 University of Edinburgh, 7 George Square, Edinburgh EH8 9JZ, UK
93 ³⁵ Department of Translational Research in Psychiatry, Max-Planck-Institute of Psychiatry,
94 Munich, Germany
95 ³⁶ ISGlobal, Barcelona Global Health Institute, Barcelona, Spain
96 ³⁷ Universitat Pompeu Fabra (UPF), Barcelona, Spain

97 ³⁸ CIBER Epidemiología y Salud Pública (CIBERESP), Madrid, Spain
98 ³⁹ Human Development and Health, Faculty of Medicine, University of Southampton,
99 Southampton, UK
100 ⁴⁰ Institute of Genetics and Molecular Medicine, University of Edinburgh, Edinburgh, UK
101 ⁴¹ INSERM UMR_S 1219, Bordeaux Population Health Center, University of Bordeaux, 33076
102 Bordeaux Cedex, France
103 ⁴² Department of General and Interventional Cardiology, University Heart Center Hamburg,
104 Hamburg, Germany
105 ⁴³ Department of Neurology, Brain Center Rudolf Magnus, University Medical Center Utrecht,
106 Utrecht, 3584 CG, The Netherlands
107 ⁴⁴ Department of Biological Psychology, Amsterdam Public Health Research Institute, Vrije
108 Universiteit Amsterdam, Van Der Boechorststraat 7-9, 1081 BT, Amsterdam, The Netherlands
109 ⁴⁵ University of Groningen, University Medical Center Groningen, Department of Pediatric
110 Pulmonology and Pediatric Allergology, Beatrix Children's Hospital, GRIAC Research Institute
111 Groningen, The Netherlands
112 ⁴⁶ Chromatin and Disease Group, Cancer Epigenetics and Biology Programme (PEBC),
113 Bellvitge Biomedical Research Institute (IDIBELL), 08908 L'Hospitalet de Llobregat, Barcelona,
114 Spain
115 ⁴⁷ Instituto de Parasitología y Biomedicina López Neyra, CSIC, Granada, Spain
116 ⁴⁸ School of Medicine and Public Health, Faculty of Medicine and Health, The University of
117 Newcastle, Newcastle, NSW, Australia
118 ⁴⁹ The Curtin/UWA Centre for Genetic Origins of Health and Disease, Faculty of Health
119 Sciences, School of Biomedical Sciences, Curtin University and School of Biomedical Sciences,
120 Faculty of Health and Medical Sciences, The University of Western Australia, Perth Australia
121 ⁵⁰ The Hospital for Sick Children, University of Toronto, Toronto, Canada M5G 1X8
122 ⁵¹ Rotman Research Institute, University of Toronto, Toronto, Canada M6A 2E1
123 ⁵² University of Essex, Wivenhoe Park, Colchester, Essex, CO4 3SQ
124 ⁵³ Department of Neurology, King's College Hospital, London, UK
125 ⁵⁴ United Kingdom Dementia Research Institute, King's College London, London, UK
126 ⁵⁵ Department of Clinical Science and Education, Södersjukhuset, Karolinska Institutet,
127 Stockholm, Sweden
128 ⁵⁶ QIMR Berghofer Medical Research Institute, Brisbane, Australia
129 ⁵⁷ Department of Psychiatry and Behavioral Sciences, Duke University Medical School, Durham,
130 NC, USA
131 ⁵⁸ Dunedin Multidisciplinary Health and Development Research Unit, Department of Psychology,
132 University of Otago, Dunedin, New Zealand
133 ⁵⁹ Program in Medical and Population Genetics, Broad Institute, Broad Institute, Cambridge, MA,
134 USA
135 ⁶⁰ MRC Social, Genetic and Developmental Psychiatry Centre, Institute of Psychiatry,
136 Psychology and Neuroscience, King's College London, London, UK
137 ⁶¹ Piemonte Centre for Cancer Prevention, Turin, Italy
138 ⁶² The Generation R Study Group, Erasmus MC, University Medical Center Rotterdam,
139 Rotterdam, The Netherlands
140 ⁶³ Department of Epidemiology, Erasmus MC, University Medical Center Rotterdam, Rotterdam,
141 The Netherlands
142 ⁶⁴ Department of Pediatrics, Erasmus MC, University Medical Center Rotterdam, Rotterdam,
143 The Netherlands
144 ⁶⁵ Department of Child and Adolescent Psychiatry, Erasmus Medical Center, Rotterdam,
145 Netherlands
146 ⁶⁶ Department of Social and Behavioral Science, Harvard TH Chan School of Public Health,
147 Boston, USA
148 ⁶⁷ School of Clinical Medicine, University of Cambridge, UK;
149 ⁶⁸ Department of Psychology, Education and Child Studies, Erasmus University
150 Rotterdam, Rotterdam, The Netherlands
151 ⁶⁹ Institute of Medical Sciences, University of Aberdeen, Aberdeen, UK

152 ⁷⁰ Department of Psychology and Logopedics, Faculty of Medicine, University of Helsinki,
153 Finland
154 ⁷¹ Research Unit for Gynaecology and Obstetrics, Institute of Clinical research, University of
155 Southern Denmark, Odense, Denmark
156 ⁷² Centre of Women's, Family and Child Health, University of South-Eastern Norway,
157 Kongsberg, Norway
158 ⁷³ The Novo Nordisk Foundation Center for Basic Metabolic Research, Faculty of Health and
159 Medical Sciences, University of Copenhagen, Denmark
160 ⁷⁴ Department of Public Health (Section of Epidemiology), Faculty of Health and Medical
161 Sciences, University of Copenhagen, Copenhagen, Denmark.
162 ⁷⁵ The National Institute of Public Health, University of Southern Denmark, Copenhagen
163 ⁷⁶ Department of Psychiatry and Behavioral Sciences, Emory University School of Medicine,
164 Atlanta, GA, USA
165 ⁷⁷ Center for Genomic Regulation (CRG), Barcelona Institute of Science and Technology,
166 Barcelona, Spain
167 ⁷⁸ IMIM (Hospital del Mar Medical Research Institute), Barcelona, Spain
168 ⁷⁹ Clinical and Experimental Sciences, Faculty of Medicine, University of Southampton,
169 Southampton, UK
170 ⁸⁰ Division of Epidemiology, Biostatistics, and Environmental Health Sciences, School of Public
171 Health, University of Memphis, Memphis, USA
172 ⁸¹ Queensland Brain Institute, University of Queensland, Australia
173 ⁸² Alzheimer Scotland Dementia Research Centre, University of Edinburgh, University of
174 Edinburgh, UK
175 ⁸³ Department of Gerontology and Geriatrics, Leiden University Medical Center, Leiden, The
176 Netherlands
177 ⁸⁴ INSERM UMR_S 1062, Nutrition Obesity and Risk of Thrombosis, Marseille, France; Aix-
178 Marseille University
179 ⁸⁵ Avera Institute for Human Genetics, Sioux Falls, USA
180 ⁸⁶ University of Groningen, University Medical Center Groningen, Department of Epidemiology,
181 GRIAC Research Institute Groningen, Groningen, The Netherlands
182 ⁸⁷ Institute for Risk Assessment Sciences, Universiteit Utrecht, Utrecht, The Netherlands
183 ⁸⁸ Julius Center for Health Sciences and Primary Care, University Medical Center Utrecht,
184 Utrecht, The Netherlands
185 ⁸⁹ Telethon Kids Institute, University of Western Australia, Perth, WA, Australia
186 ⁹⁰ UCL Institute of Cardiovascular Science, London, UK
187 ⁹¹ Bloorview Research Institute, Holland Bloorview Kids Rehabilitation Hospital and
188 Departments of Psychology and Psychiatry, University of Toronto, Toronto, Canada, M4G 1R8

189 Contributions

190 **Project management:** G.S., J.L.M

191 **Designed individual studies and contributed data:**

192 A.A.C., A.Cas., A.D.H., A.G.U, A.Me., A.Mu., A.M.M., B.B., B.T.H.,
193 C.H., C.L.R., C.P., C.Sa., C.Sh., C.Sö., D.A.L., D.v.H., D.I.B., D.T., E.A.N., E.B.B., E.J.C.d.G,
194 E.M., F.G., F.R., G.E.D, G.H.K., G.P., G.W.M., H.R.E., H.T., H.Z., I.J.D., J.F.F., J.H.V., J.J.C.,
195 J.Ka., J.L., J.M., J.M.S., J.M.V., J.v.M., J.R., J.R.B.P., J.R.G., J.Sh., J.T.B., J.W., J.W.H.,
196 K.K.O., K.L.E., K.R., L.A., L.C.S., L.M., M.A.I., M.Bee., M.Bu., M.E.A.R., M.H.v.IJ., M.Ke., M.O.,
197 N.C., N.G.M., N.J.W., N.R.W., P.E.S., P.Mo., P.M.V., R.H., R.P., S.L., T.D.S., T.E., T.E.M.,
198 T.I.A.S, T.P., T.T., V.W.V.J., W.K., Z.P.

199 **Generated and/or quality-controlled data:** A.A.K., A.I., A.S., C.S.M., H.R.E., J.L.M., K.B.,
200 K.M.H., N.K., S.M.R., T.H., R.M.W., W.L.M.

201 **Designed new statistical or bioinformatics tools:** G.H., J.L.M., M.Su., T.R.G., V.I.

202 **Analysed the data and/or provided critical interpretation of results:**

203 A.D.B, A.Car., A.D., A.F.M., A.K., B.T.H., C.B., C.H., C.L.R., C.R.A., C.Sor., C.V., C.X., C.W.,
204 D.A., D.C., D.J.L., D.L.C., D.M., E.C.M., E.G., E.H., E.M., F.C.M., F.I.R., F.R.D., G.B., G.C.,
205 G.D.S., G.H., G.H.K., G.M., G.W., I.Y., J.C.F., J.v.D., J.J.H., J.Ka., J.Kl., J.L.M., J.M., J.Su.,
206 J.T.B., K.B., K.v.E., K.F.D., K.S., L.C.S., M.Ber., M.Bu., M.H.v.IJ., M.G., M.Ku., M.L., M.Sm.,
207 M.Su., N.K., P.Me., P.Ma., P.M.V., R.E.M., R.G., R.L., R.Z., S.B., S.G., S.K., T.C., T.G., T.G.R.,
208 T.I.A.S., T.L., T.R.G., Y.A., Y.Z., V.I., V.S.
209 **Designed and/or managed the study:** B.T.H., C.B., C.L.R., J.M., J.T.B., T.R.G.
210 **Wrote the manuscript:** A.D.B., B.T.H., C.B., C.L.R., D.J.L., E.C.M., E.H., G.D.S., G.H., J.C.F.,
211 J.Kl., J.L.M., J.M., J.T.B., K.B., K.F.D., M.Su., P.M.V., R.L., T.G.R., T.R.G., V.I.

212 Competing interests

213 The authors declare no competing interests.

214 Financial disclosures

215 None of the authors have financial disclosures.

216

217 Abstract

218 Characterizing genetic influences on DNA methylation (DNAm) provides an opportunity to
219 understand mechanisms underpinning gene regulation and disease. Here we describe results of
220 DNA methylation-quantitative trait loci (mQTL) analyses on 32,851 participants, identifying
221 genetic variants associated with DNAm at 420,509 DNAm sites in blood. We present a
222 database of >270,000 independent mQTL of which 8.5% comprise long-range (*trans*)
223 associations. Identified mQTL associations explain 15-17% of the additive genetic variance of
224 DNAm. We reveal that the genetic architecture of DNAm levels is highly polygenic and DNAm
225 exhibits signatures of negative and positive natural selection. Using shared genetic control
226 between distal DNAm sites we construct networks, identifying 405 discrete genomic
227 communities enriched for genomic annotations and complex traits. Shared genetic factors are
228 associated with both blood DNAm levels and complex diseases but in most cases these
229 associations do not reflect causal relationships from DNAm to trait or vice versa indicating a
230 more complex genotype-phenotype map than has previously been hypothesised.

231 Main

232 The role of inter-individual variation in DNA methylation (DNAm) on disease mechanisms is not
233 yet well characterised. It has, however, been hypothesised to serve as a viable biomarker for
234 risk stratification, early disease detection and the prediction of disease prognosis and
235 progression¹. Because genetic influences on DNAm have been shown to be widespread^{2,3,4}, a
236 powerful avenue into researching the functional consequences of changes in DNAm levels is to
237 map genetic differences associated with population-level variation, identifying DNA methylation
238 quantitative trait loci, (mQTL) that include both local (*cis* mQTL) and distal (*trans* mQTL) effects.
239 We can harness mQTL as natural experiments, allowing us to observe randomly perturbed
240 DNAm levels in a manner that is not confounded with environmental factors^{5,6}. In this regard,

241 mapping even very small genetic effects on DNAm is valuable for gaining power to evaluate
242 whether its variation has a substantial causal role in disease and other biological processes.

243
244 To date, only a small fraction of the total genetic variation estimated to influence DNAm across
245 the genome has been identified, primarily restricted to *cis* mQTL⁷. Yet the majority of genetic
246 effects are likely to act in *trans* (defined as more than 1Mb from the DNAm site) and have small
247 effect sizes^{5,7-9}. As with classical complex traits¹⁰, much larger sample sizes are required to map
248 associations involving small genetic effects in order to permit greater understanding of the
249 genetic architecture and the biological processes underlying DNAm⁷. To this end, we
250 established the Genetics of DNA Methylation Consortium (GoDMC), an international
251 collaboration of human epidemiological studies that comprises >30,000 study participants with
252 genetic, phenotypic and DNAm data.

253
254 Importantly, the unrivalled sample size and coverage of our study enables us to identify a large
255 number of *cis* and *trans* mQTL to gain biological insights that were previously impossible. First,
256 we use this extensive resource to uncover the genetic architecture of DNAm and to study
257 natural selection pressures. Second, we learn about how *cis*- and *trans*-acting variants and
258 DNAm sites interact through the development of new network approaches. Third, we interrogate
259 the potential role of DNAm in disease mechanisms by exhaustively mapping the causal
260 relationships of DNAm with 116 complex traits and diseases in a bi-directional manner. A
261 database of our results is available as a resource to the community at
262 <http://mqtl.db.godmc.org.uk/login.php> (username: godmc; password: GreatestHits1)

263 Genetic variants influence 45% of tested DNAm sites

264 In order to map genetic influences on DNAm, we established an analysis workflow that enabled
265 standardized meta-analysis and data integration across 36 population-based and disease
266 datasets with genotype and DNAm data. Using a two-phase discovery study design, we
267 analyzed ~10 million genotypes imputed to the 1000 Genomes reference panel¹¹ and 420,509
268 DNAm sites measured by Infinium HumanMethylation BeadChips in whole blood derived from
269 27,750 European participants (**Figures 1A** and **S1-S5**, **Table S1-S2**, **Supplementary Note 1**,
270 **Supplementary Information**).

271
272 Using linkage disequilibrium (LD) clumping, we identified 248,607 independent *cis*-mQTL
273 associations ($p < 1e-8$, < 1Mb from the DNAm site, **Figure S4**) with a median distance between
274 single nucleotide polymorphisms (SNP) and DNAm sites of 36kb (IQR=118 kb, **Figure S3A**).
275 We found 23,117 independent *trans* mQTL associations (using a conservative threshold of $p <$
276 $1e-14$ ⁷, **Figure S4**, **Supplementary Information**). These mQTL involved 190,102 DNAm sites,
277 representing 45.2% of all those tested (**Figure 1B**) which is a 1.9x increase of sites with a *cis*
278 association ($p < 1e-8$) and 10x increase of sites with a *trans* association ($p < 1e-14$) over a
279 previous study whose sample size was 7x smaller⁸. As expected, mQTL effect sizes for each
280 DNAm site (the maximum absolute additive change in DNAm level measured in standard
281 deviation (SD) per allele) were lower for sites with a *trans* association (as compared to sites with
282 a *cis* association (per allele SD change = -0.02 (s.e.=0.002, $p=2.1e-14$, **Figure S6**). The
283 differential improvement in yield between *cis* and *trans* associations is revealing in terms of the
284 genetic architecture – relatively small sample sizes are sufficient to uncover the majority of large

285 *cis* effects, whereas much larger sample sizes are required to identify the polygenic *trans*
286 component.

287
288 The majority of *trans* associations (80%) were inter-chromosomal. Of the intra-chromosomal
289 *trans* associations, 34% were >5 Mb from the DNAm site, **Figure S7**). We then compared the
290 rate of inter-chromosomal *trans* associations to the rate of intra-chromosomal *trans* associations
291 (excluding chromosome 6) and found a substantially lower number of inter-chromosomal *trans*
292 associations per 5 Mb region (1.59) than intra-chromosomal associations (>1 Mb: 7.95; >6 Mb
293 4.81).

294
295 Next, using conditional analysis¹² we explored the potential for multiple independent SNPs
296 operating within the locus of each mQTL, identifying 758,130 putative independent variants.
297 Each DNAm site, for which a mQTL in *cis* had been detected, had a median of 2 independent
298 variants (IQR=4 variants, **Figure S8**). For all subsequent analyses, we used index SNPs from
299 clumping procedures to be conservative and unbiased due to the non-independence of genetic
300 variants.

301
302 We sought to replicate these mQTL using the Generation Scotland (GS) cohort (n = 5,101) for
303 which mQTL results were previously generated using an independent analysis pipeline
304 (**Supplementary Information, Supplementary Note 1**). Data were available to allow us to test
305 for replication of 188,017 of our discovery mQTL (137,709 sites) and we found a very strong
306 correlation of effect sizes for both *cis* and *trans* effects ($r=0.97$, $n=155,191$ and 0.96 , $n=14,465$
307 at $p<1e-3$, respectively; **Figure 1C**); 99.6% of the associations had a consistent sign (further
308 discussion in **Supplementary Information**). At an approximate Bonferroni corrected threshold
309 of $0.05/188,017$, 142,727 of the discovery mQTL replicated in the GS cohort (76%); the
310 replication rate for *cis* and *trans* mQTL were 76% and 79%, respectively. To evaluate whether
311 our replication rate was in line with expectations given the smaller replication sample size, we
312 estimated that under the assumption that the discovery mQTL are true positives 171,824 mQTL
313 would be expected to replicate at a nominal threshold of $1e-3$. In very close agreement we
314 found that the actual number of mQTL replicating at this level was 169,656, indicating that the
315 majority of our discovery mQTL are likely to be true positives (**Table S3, Supplementary**
316 **Information**). Our findings support that there is little between-study heterogeneity in our
317 analysis and that genetic effects on DNAm are highly stable across cohorts (**Figure S2, Table**
318 **S2**).

319
320 Overall the variance explained by replicated genetic effects was small. For 99% of the
321 associations in *cis* and *trans*, mQTL explained less than 21% and 16% of the DNAm variation
322 respectively (**Figure S9**). Aggregating across all 420,509 tested DNAm sites, our replicated
323 mQTL associations explain 1.3% of the total assayed DNAm variation, 8% of this being due to
324 *trans*-associations. Restricting to sites that have at least one *cis*-effect or *trans*-effect, however,
325 we explain 4.2% and 2.5% of the DNAm variance, respectively.

326
327 We then investigated how much of the heritability of variable DNAm can be explained by mQTL
328 associations in GoDMC using family-based heritability studies of DNAm^{2,3}. We found a strong
329 positive relationship between variance explained by replication mQTL estimates (127,680 sites
330 in GS) and heritability for both studies (family: $r=0.41$ across, 121,582 available sites; twin:
331 $r=0.37$ across 118,955 available sites) (**Figure 1D, Table S4**). The mQTL that we identified
332 explain 15%-17% of the additive genetic variance of DNAm (**Figure S10**). Finally, there were

333 strong positive relationships between the heritability of DNAm levels at a DNAm site and the
334 number of independent mQTL (**Figure S11**), heritability and effect size (**Figure S12**), variance
335 explained and the number of independent mQTL (**Figure S13**) and variance explained and
336 distribution of DNAm levels (**Figure S14**). Overall, our results support a mixed genetic
337 architecture of polygenic genome-wide effects and larger *cis* effects.

338 *Cis* and *trans* mQTL operate through distinct mechanisms

339 DNAm is usually associated with gene repression, with loss of DNAm reflecting enhancer or
340 gene activation¹³⁻¹⁵. We analysed how interindividual DNAm changes are associated to genetic
341 variation in a context way which has so far mainly focused on *cis* mQTL^{7,8,16,17,19}. The statistical
342 power of the mQTL analysis allowed us to identify SNPs only associated with DNAm in *cis*
343 (n=157,095, 69.9%), only associated with DNAm in *trans* (n=794, 0.35%), or associated with
344 DNAm in both *cis* and *trans* (n=66,759, 29.7%). Similarly, of the 190,102 DNAm sites influenced
345 by a SNP, 170,986 DNAm sites (89.9%) were *cis-only*, 11,902 DNAm sites (6.3%) were
346 *cis+trans*, and 7,214 DNAm sites (3.8%) were *trans-only*. This categorisation allowed us to infer
347 biological properties of *trans*-features that were not due to their *cis*-effects.

348
349 Here, we first compared the distribution of DNAm levels (weighted mean DNAm level across 36
350 studies (defined as low (<20%), intermediate (20%-80%) or high (>80%) between the *cis* and
351 *trans* DNAm sites (**Figure 1B**). We then performed enrichment analyses on the mQTL SNPs
352 and DNAm sites using 25 combinatorial chromatin states from 127 cell types (including 27 blood
353 cell types)¹⁸ and gene annotations (**Figure 2A, S15-S18, Tables S5-S8**). Consistent with
354 previous studies^{7,8,19}, we found that *cis only* sites are represented in high (32%), low (28%) and
355 intermediate (40%) DNAm levels and these sites are mainly enriched for enhancer chromatin
356 states (mean OR=1.37), CpG islands (OR=1.25) and shores (OR=1.26).
357 For *cis+trans* sites, we found that the majority of these sites (66%) have intermediate DNAm
358 levels. By replicating this finding in two isolated white-blood-cell subsets, we showed that this is
359 due to cell-to-cell variability^{18,20} and not explained by between cell type differences (**Figure**
360 **S19**). In line with the observation that intermediate levels of DNAm are found at distal regulatory
361 sequences^{21,24}, these sites were enriched for enhancer (mean OR=1.65) and promoter states
362 (mean OR=1.41). However for *trans only* sites, we found a pattern of low DNAm (for 55% of
363 sites) and enrichments for promoter states (mean OR=1.39) especially TssA promoter state
364 (mean OR=2.03). We demonstrated that these inferences about *cis* and *trans* enrichments were
365 not sensitive to the definition of *trans* associations, by showing that the patterns were consistent
366 if we restricted to only inter-chromosomal associations (**Supplemental Information, Figure**
367 **S20**).

368
369 We continued by analysing the differences in properties between SNPs that have local versus
370 long-range DNAm influences. We found that *cis only* and *cis+trans* SNPs were enriched for
371 active chromatin states and genic regions whereas *trans only* SNPs were enriched for intergenic
372 regions and the heterochromatin state (**Figure 2A, S17-S18, Tables S7-S8**). This implies that
373 the enrichments for the *cis+trans* SNPs were driven by their *cis* signals. Overall, these results
374 highlight that a complex relationship between molecular features is underlying the mQTL
375 categories and the biological contexts are substantially different between *cis* and *trans* features.

376

377 We found that these inferences were often shared across other tissues. For example, DNAm
378 sites with low or intermediate DNAm levels have similar DNAm distributions in 12 tissues
379 (**Figure S21-23**). However, while SNP and DNAm site enrichments were typically present in
380 multiple tissues, enrichments were stronger in blood datasets for the enhancer states (SNP:
381 difference in mean OR=0.055, $p=0.038$; sites: difference in mean OR=0.21, $p < 2e-16$) and
382 DNase state (SNP: difference in mean OR=0.13, $p=0.004$; sites: difference in mean OR=0.41
383 $p=9.65e-16$) indicating some level of tissue specificity for mQTL in these regions (**Figure S15,**
384 **S17, S24**).

385
386 To investigate the question of tissue specificity further, we compared the correlation of effect
387 estimates of *cis* and *trans* mQTL in blood against adipose tissue ($n=603$)²² and brain ($n=170$)⁹
388 (**Supplementary Information, Table S9**). Generally, the between tissue effect correlations
389 were high, in line with a recent comparison of *cis*-mQTL effects between brain and blood²³.
390 However, we found that the highest correlations were for associations involving *trans-only* sites
391 (Adipose $r_b=0.92$ (se =0.004); Brain $r_b=0.88$ (se=0.009)) despite having on average smaller
392 effect sizes than *cis only* associations, implying that they are *less* tissue specific than *cis* effects
393 (Adipose $r_b=0.73$ (se =0.002); Brain $r_b=0.59$ (se=0.004)). Stratifying the mQTL categories to low,
394 intermediate and high DNAm, showed that the brain-blood correlations are the lowest for
395 intermediate DNAm categories and adipose-blood correlations are lowest for high DNAm
396 categories, which may suggest cellular heterogeneity for high DNAm levels (**Table S9**). These
397 results show the value of large sample sizes in blood to detect *trans* mQTL regardless of the
398 tissue.

399 *Trans* mQTL SNPs and DNAm exhibit patterned TF binding

400 Binding of transcription factor (TF) to distal regulatory elements correlates with low DNAm levels
401 and regulates gene activity^{24,25}. To gain insights into how SNPs induce long-range DNAm
402 changes, we mapped enrichments for DNAm sites and SNPs across binding sites for 171 TFs in
403 27 cell types^{26,27}. We found strong enrichments for the majority of TFs amongst DNAm sites with
404 a *trans* association (*cis+trans*: 55%; *trans only*: 80%; *cis only*: 18%) and amongst *cis-acting*
405 SNPs (*cis only*: 96%, *cis+trans*: 91%, *trans only*: 1%) (**Figures 2B, S25, S26**). Sites that overlap
406 TFBS were relatively hypomethylated independent of tissue (weighted mean DNAm levels =
407 21% vs 52%, $p<2.2e-16$) (**Figure S27**) and we found that generally the TFBS enrichments were
408 not tissue specific (**Table S10-11, Figure S25-26**). Overall, these enrichments illustrate multiple
409 mechanisms at play: that marginally the *trans* associations are not arising due to direct genetic
410 influences on TF activity, whereas *cis* associations could be. It therefore raises the question,
411 what is the relationship between the TFBS occupancy of a DNAm site and a SNP in a *trans*-
412 mQTL?

413
414 The enrichment analyses above have focused on analysing mQTL SNPs and mQTL sites
415 marginally. However, a mQTL has a pair of TFBS annotations²⁶, one for the SNP and one for
416 the DNAm site, and they can be analysed for joint pairwise enrichment. Using a novel approach
417 (two-dimensional functional enrichment, **Figure S28**), we evaluated if the annotation pairs
418 amongst 18,584 inter-chromosomal *trans*-mQTL were associated to TF binding in a non-random
419 pattern (**Supplementary Information**). We found that across the *trans*-mQTL there was
420 substantial non-random pairing of TFBS annotations for DNAm sites and SNPs. We found that
421 6.1% (22,962 of 378,225) of possible pairwise combinations of SNP-DNAm site annotations

422 were more over- or under-represented than expected by chance after strict multiple testing
423 correction (**Supplementary Information, Table S12, Figure 2C-D**).

424
425 After accounting for abundance and other characteristics, the strongest pairwise enrichments
426 involved sites close to TFBS for proteins in the cohesin complex, for example CTCF, SMC3 and
427 RAD21, as well as TFs such as GATA2 related to cohesin²⁸. Bipartite analysis showed that
428 these clustered due to being related to similar sets of SNP annotations (**Figure 2C**). Other
429 clusters were also found, for example, sites close to TFBS for interferon regulatory factor 1
430 (*IRF1*), a gene for which *trans*-acting regulatory networks have been previously reported²⁹, were
431 more likely to be influenced by SNPs near TFBS for EZH2, SMC3, ATF3, BCL3, TR4 and MAX.
432 The relationship between IRF1 and these other proteins has been documented previously^{30–32}.
433 For example EZH2 mediates the silencing of IRF1³³; BCL3 and IRF1 are co-down-regulated
434 during inflammation³⁰; and ATF3 is a negative regulator of cytokines which themselves induce
435 IRF1^{31,32}.

436
437 To further investigate mechanisms by which inter-chromosomal *trans* mQTL (n=18,584) can
438 arise, we compared their locations to known regions of chromosomal interactions (genomic
439 regions that have been shown to spatially colocalise within the cell³⁴). We found 1175 overlaps
440 for 637 SNP-DNA site pairs (3.4%) where the LD region of the mQTL SNP and the
441 corresponding site overlapped with any interacting regions (525 SNPs, 602 sites) as compared
442 to a mean of 473 SNP-DNA site pairs in 1000 permuted datasets (OR=1.36, $p_{\text{Fisher}}=6.5e-7$,
443 $p_{\text{empirical}} < 1e-3$) (**Figure S29**). To summarise, the order of operation between transcription factor
444 (TF) binding and demethylation requires further investigation^{8,25,16}, but these results indicate that
445 for a small proportion of interchromosomal *trans* mQTL the spatial distance *in vivo* is likely to be
446 small.

447 Communities of DNAm sites are identified by shared *trans*-genetic 448 effects

449 *Trans*-mQTL provide an opportunity to infer how distal genomic regions are functionally related,
450 but the polygenic nature of DNAm variation could lead to apparent shared genetic effects that
451 arise from distinct causal variants rather than shared genetic factors. We observed that there
452 were 1,728,873 instances where a SNP acting in *trans* also influenced a *cis* DNAm site (before
453 LD pruning). Genetic colocalization analysis indicated that 278,051 of these instances were due
454 to the *cis* and *trans* sites sharing a genetic factor, representing 3,573 independent *cis-trans*
455 genomic region pairs, of which 3,270 were inter-chromosomal (**Table S13**). These pairs
456 consisted of 1,755 independent SNPs and 5,109 independent DNAm sites across the genome,
457 indicating that some sites with *cis* associations shared genetic factors with multiple sites with
458 *trans* associations. From the *cis-trans* pairs we constructed a network linking these genomic
459 regions which elucidated 405 “communities” of genomic regions that were substantially
460 connected (**Supplementary Information**). Fifty-six of these communities comprised 10 or more
461 sites, and the largest community comprised 253 sites (**Figure 3A**).

462
463 We hypothesised that *cis* sites were causally influencing multiple *trans* sites within their
464 communities (i.e. a causal chain of mQTL to DNAm at a *cis* site to DNAm at a *trans* site). We
465 evaluated whether the estimated causal effect (obtained from the *trans*-mQTL effect divided by
466 the *cis*-mQTL effect i.e. the Wald ratio) of the *cis* site on the *trans* site was consistent with the

467 observational correlation between the *cis*- and *trans*-site. While there was an association, the
468 relationship was weak ($r=0.096$, $p=1.73e-6$, **Figure S30**), indicating that changes in *cis* sites
469 causing changes in *trans* sites is likely not the predominant mechanism. We did observe that
470 the *cis-trans* DNAm levels were more strongly correlated than we would expect by chance
471 (**Figure S31**), which supports the notion that they are jointly regulated without generally being
472 causally related.

473
474 To gain functional insights into these communities, we evaluated if DNAm sites within
475 communities were enriched for regulatory annotations and/or gene ontologies (**Table S14-S17**,
476 **Figure S32-33**). Multiple communities showed enrichments (FDR $P < 0.001$); for example
477 community 9 sites were strongly enriched for TFBS annotations relating to the cohesin complex
478 in multiple cell types, community 22 sites were enriched for NFKB and EBF1 in B lymphocytes
479 and community 76 sites were enriched for EZH2 and SUZ12 and bivalent promotor and
480 repressed polycomb states (**Figure 3B**). Community 2 (comprising 253 sites) was enriched for
481 active enhancer state in 3 cell types and for lymphocyte activation (GO:0046649 FDR $p =$
482 0.016) and multiple KEGG pathways including the JAK-STAT signalling pathway (I04630: FDR
483 $p=8.53e-7$) (**Table S16, Table S17**).

484
485 Regulatory features within a network may share a set of biological features that are related to
486 complex traits. We performed enrichment analysis to evaluate if the loci tagged by DNAm sites
487 in a community were related to each of 133 complex traits (**Table S18**), accounting for non-
488 random genomic properties of the selected loci. Restricting the analysis to only the 56
489 communities with ten or more sites, we found eleven communities that tagged genomic loci that
490 were enriched for small p -values with 22 complex traits (FDR < 0.05) (**Figure 3C, Table S19**).
491 Blood related phenotypes were overrepresented (11 out of 23 enrichments being related to
492 metal levels or haematological measures, binomial test p -value = $4.2e-5$). Amongst the
493 communities enriched for GWAS signals, community 16 was highly associated with iron and
494 haemoglobin traits. Community 9 was associated to plasma cortisol ($p = 8.27e-5$). Finally, we
495 performed enrichment analysis on 36 blood cell count traits³⁵ and found enrichments for two
496 communities. Community 16 was enriched for hematocrit ($p=4.34e-10$) and hemoglobin
497 concentration ($p=1.99e-8$) and community 5 was enriched for reticulocyte traits ($p=1.67e-6$)
498 (**Figure S34**). The enrichments found for these DNAm communities indicate that a potentially
499 valuable utility of mapping *trans*-mQTL is to indicate how distal regions of the genome are
500 functionally related independent from cellular composition.

501 mQTL can be used to identify shared genetic influences with 502 disease

503 The majority of GWA loci map to non-coding regions³⁶ and *cis* mQTL are enriched amongst
504 GWA^{17,37,38}. Here we investigated the value of the large number of mQTL especially *trans* mQTL
505 to annotate functional consequences of GWA loci. We first tested genome-wide enrichment of
506 GWAS associations (SNPs at $p < 5e-8$ for a given complex trait) amongst mQTL SNPs,
507 performing separate analysis for mQTL acting in *cis*, *cis* and *trans* and *trans*. We utilized
508 genome-wide summary statistics for 37 phenotypes related to 11 disease/trait categories with
509 41 publicly available GWAS datasets (**Table S20**). After accounting for non-random genomic
510 distribution of mQTL³⁹ and multiple testing, we identified enrichments for 35% of the complex
511 traits (**Figure S35, Table S20, Supplementary Information**) mainly for studies with a larger

512 number of GWA signals. The *cis+trans* mQTL were most strongly enriched for low p-values
513 across multiple traits. Six phenotypes across 4 disease categories were associated with *cis*
514 mQTL, nine phenotypes across 5 disease categories were associated with *cis+trans* mQTL.
515 Inflammatory bowel disease and Crohn's disease were associated with both sets. Height was
516 associated across all three categories of mQTL but interestingly was depleted for mQTL in the
517 *trans only* group (OR=0.354, p=7.31e-8). The distribution of enrichment effect estimates (ORs)
518 of *trans* mQTL was substantially closer to the null or in depletion when compared to mQTL that
519 included *cis* effects (**Figure 2E**). These enrichments correspond to the results reported earlier,
520 in which *trans*-SNPs were typically found in intergenic regions, which are known to be depleted
521 for complex trait loci⁴⁰.

522
523 Though the mQTL discovery pipeline adjusted for predicted cell types^{41,42} and non-genetic
524 DNAm PCs, there is a possibility that residual cell-type heterogeneity remains. We performed
525 another set of GWAS enrichment analysis, this time using 36 blood cell traits³⁵, and found
526 enrichments. These were strongest amongst *cis+trans* mQTL, as seen in the previous
527 enrichments (**Figure S36**). Interrogating this further, we found that for 98.9-100% of the mQTL,
528 mQTL SNPs explained more variation in DNAm than they explain variation in blood cell counts
529 suggesting a causal chain of mQTL to blood trait⁴³. Alternatively, a systematic measurement
530 error difference could explain these observations, where DNAm captures blood cell counts more
531 accurately than conventional measures.

532
533 The enrichments suggest that overlaps are not due to chance which motivated us to a much
534 more in-depth analysis on a much larger number of traits/diseases. We searched for instances
535 of DNAm sites sharing the same genetic factors against each of 116 complex traits and
536 diseases, and initially found 23,139 instances of an mQTL strongly associating with a complex
537 trait (**Figure 4**). To evaluate the extent to which these were due to shared genetic factors (and
538 not, for example, LD between independent causal variants), we performed genetic
539 colocalization analysis⁴⁴ (**Table S18, Table S21**). Excluding genetic variants in the *MHC* region,
540 we found 1,373 putative examples in which at least one DNAm site putatively shared a genetic
541 factor with at least one of 71 traits (including 19 diseases). Those DNAm sites that had a shared
542 genetic factor with a trait were 6.9 times more likely to be present in a community compared to
543 any other DNAm site with a known mQTL (Fisher's exact test 95% CI 4.8-9.7, p =9.2e-19). Next,
544 we evaluated how often the DNAm site that colocalised with a known GWAS hit was the closest
545 DNAm site to the lead GWAS variant by physical distance. Notably, in only 18.1% of the cases
546 where a GWAS signal and a DNAm site colocalised, was that DNAm site the closest DNAm site
547 to the signal. This finding is similar to results found for gene expression⁴⁵, but the converse has
548 been found for protein levels⁴⁶.

549
550 It has previously been difficult to conclude whether genetic colocalisation between DNAm and
551 complex traits indicates a) a causal relationship where the DNAm level is on the pathway from
552 genetic variant to trait (vertical pleiotropy) or b) a non-causal relationship where the variant
553 influences the trait and DNAm independently through different pathways (horizontal
554 pleiotropy)⁴⁷. In Mendelian randomisation (MR) it is reasoned that under a causal model,
555 multiple independent genetic variants influencing DNAm should exhibit consistent causal effects
556 on the complex trait⁴⁸. Amongst the putative colocalising signals, 440 (32%) involved a DNAm
557 site that had at least one other independent mQTL. To test if there was a general trend of
558 DNAm sites causally influencing a trait, we evaluated if the MR effect estimate based on the
559 colocalising signals were consistent with those obtained based on the secondary signals. There

560 were substantially more large genetic effects of the secondary mQTL on respective traits than
561 expected by chance (70 with $p < 0.05$, binomial test $p = 2.4e-16$). However only 41 (59%) of
562 these had effect estimates in the same direction as the primary colocalising variant, which is not
563 substantially better than chance (binomial test $p = 0.19$). Twelve of the 41 mQTL were located in
564 the *HLA* region. Of the remaining mQTL, 27 were associated with anthropometric (*ESR1* and
565 birth weight), immune response (*IRF5* and systemic lupus erythematosus) and lipid traits (*TBL2*
566 and triglycerides). We then performed systematic colocalization analysis of all mQTL against 36
567 blood cell traits³⁵. Here we discovered 94,738 instances of a DNAm site and a blood cell trait
568 sharing a causal variant. In 28,138 instances the colocalising DNAm site had an independent
569 secondary mQTL, and with these associations we again tested for a general trend of DNAm
570 sites causally influencing the blood trait. The association between primary and secondary
571 signals was very weak ($R^2 = 0.008$), suggesting that the general causal model is not supported.
572 Together, these results indicate that those blood measured DNAm sites that have shared
573 genetic factors with traits cannot be typically thought of as mediating the genetic association to
574 the trait (**Figure S37-S38, Table S22**). Instead, if DNAm is a coregulatory phenomenon then the
575 colocalising signals between DNAm sites and complex traits may be due to a common cause,
576 for example genetic variants primarily acting on TF binding^{8,49,50}.

577 The influence of traits on DNAm variation

578 Previous studies have not been adequately powered to estimate the causal influences of
579 complex traits on DNAm variation through MR, as the sample size of the outcome variable
580 (DNAm) is a predominant factor in statistical power^{44,51}. We systematically analysed 109 traits
581 for causal effects on DNAm using two-sample MR^{52,53}, where each trait was instrumented using
582 SNPs obtained from their respective previously published GWAS (**Supplemental Note 2, Table**
583 **S18**). Included amongst the traits were 35 disease traits, which when used as exposure
584 variables in MR must be interpreted in terms of the influence of liability rather than
585 presence/absence of disease. The sample size used to estimate SNP effects in DNAm was up
586 to 27,750 (**Figure 4**).

587
588 We initially identified 4785 associations where risk factors or genetic liability to disease
589 influences DNAm levels (multiple testing threshold $p < 1.4e-7$). However, MR analysis on omic
590 variables can lead to false positives due to violations in assumptions. We developed a filtering
591 process involving a novel causal inference method to help protect against these invalid
592 associations (**Supplementary Information, Supplementary Note 2, Figure S39**). This left 85
593 associations (involving 84 DNAm sites) in which DNAm sites were putatively influenced by 13
594 traits (nine risk factors or four diseases) (**Table S23**). Further filtering that would exclude traits
595 that were predominantly instrumented by variants in the *HLA* region or driven by one SNP would
596 reduce the total number of associations substantially from 84 to 19. We replicated five
597 associations for triglycerides influencing DNAm sites near *CPTA1* and *ABCG1*⁵⁴ and found
598 associations for transferrin saturation/iron influencing DNAm sites near *HFE*.

599
600 We next evaluated if there was evidence for small, widespread changes in DNAm levels in
601 response to complex trait variation, by calculating the genomic control inflation factor (GC_{in}) for
602 the p-values obtained from the MR analyses of each trait against all DNAm sites. Five traits
603 (fasting glucose, age at menarche, cigarettes smoked per day, immunoglobulin G index levels,
604 serum creatinine), showed GC_{in} values above 1.05 (**Figure S40**). A high GC_{in} value can be the

605 result of the trait that has an influence on a few sites or has a widespread effect on DNAm. GC_{in}
606 calculations were performed at each chromosome singly for each trait (**Figure S41**) and in a
607 leave-one-chromosome-out analysis (**Figure S42**). The GC_{in} remained consistent (except for
608 immunoglobulin G index levels), indicating that the traits have small but widespread influences
609 on DNAm levels across the genome.

610
611 While most of the traits ($n=105$, 96%) tested did not appear to induce genome-wide enrichment
612 this does not rule out the possibility of them having many localised small effects. For example,
613 the smallest MR p-value for the analysis of body mass index on DNAm levels was $2.27e-6$,
614 which did not withstand genome-wide multiple testing correction, and GC_{in} was 0.95. However,
615 restricting GC_{in} to 187 sites known to associate with body mass index from previous epigenome-
616 wide association studies (EWAS)²⁰ indicated a strong enrichment of low p-values (median GC_{in}
617 = 3.95). A similar pattern was found for triglycerides, in which genome-wide median GC_{in} = 0.94
618 but the 10 sites known to associate with triglycerides from previous EWAS⁵⁵ had an MR p-value
619 of $8.3e-70$ (Fisher's combined probability test). These results indicate that traits causally
620 influencing DNAm levels in blood is the most likely mechanism that gives rise to these EWAS
621 hits. It also indicates that the general finding that there were very few filtered putative causal
622 effects of risk factors or genetic liability to disease on DNAm could be due to true positives
623 being generally very small, even to the extent that our sample size of up to 27,750 individuals
624 was insufficient to find them.

625 DNAm sites influenced by genetic variation are under selection

626 Natural selection has modified the allele frequency of complex trait associated variants through
627 their beneficial or deleterious effects on fitness^{56,57,58,59}. Here we investigate whether mQTL
628 SNPs are frequent targets of natural selection utilizing selection scores acting through different
629 timescales and mechanisms to each SNP in 1000G: a population differentiation method (global
630 F_{st}), several haplotype-based methods (integrated haplotype score (iHS), Cross Population
631 Extended Haplotype Homozygosity (XPEHH) and the singleton density score (SDS) (**Table**
632 **S24, Supplementary Information**).

633
634 We then tested whether there is enrichment of mQTL associations (Bonferroni adjusted p
635 <0.01) among SNPs that show evidence of positive selection for each metric while controlling
636 for non-random genomic distribution³⁹ (excluding two regions (*HLA* and *LCT*) known to be under
637 high selective pressure). We found enrichments of positive selection signatures among SNPs
638 with *cis only* (F_{st} : $p=7.87e-23$, OR=1.31, SDS: $p=4.43e-10$, OR=1.42) and *cis+trans* (F_{st} : $p=7.1e-$
639 21 , OR=1.35, SDS: $p=4.35e-11$, OR=1.53, XPEHH (CEU vs CHB): $p=7.7e-7$, OR=1.53)
640 associations (**Figure 2F, Table S25**). The strong enrichments for *cis+trans* ($n=107-1585$) and
641 *cis only* ($n=1186-4980$) indicating that positive selection is most likely to operate on *cis* acting
642 variants. However, there is less power to detect these enrichments for *trans only* SNPs ($n=14-$
643 102).

644
645 We next examined whether there was a relationship between the mQTL effect sizes (allele
646 frequency adjusted) and the selection scores as a proxy for the estimated strength of selection.
647 Using a linear model for each of the selection metrics (accounting for the number of proxies,
648 distance to TSS, CpG and GC frequency), we found that the strongest mQTL effect size was
649 positively associated with F_{st} ($p<1.1e-05$) but not with recent changes in allele frequency

650 (measured by SDS) with consistent directions across the mQTL categories (*cis only*, *cis+trans*
651 and *trans only*) (**Figure S43**). These results may indicate that DNA sites might either the
652 primary target of selection or the mQTL SNP have pleiotropic effects on fitness⁶⁰.

653
654 Enrichment of F_{st} amongst mQTL could also be due to negative selection. Evidence for negative
655 selection can be inferred from the strong negative relationship between mQTL SNP effect size
656 and MAF (difference in mQTL SNP effect size=-0.56, $p=2.2e-308$, **Figure S43**). To confirm that
657 this relationship is not an artefact of having defined the SNP effect via the maximum effect each
658 SNP has on any DNAm site, we developed a novel method (**Supplementary Information**,
659 **Figure S44**) to quantify the relationship for the strongest acting SNPs at a given frequency,
660 allowing for a majority of unselected SNPs. SNPs with a higher frequency have a smaller
661 average effect ($S=0.4$, CI 0.325-0.475), where $S=0$ corresponds to no selection and $S=1$
662 corresponds to strong negative selection. We found similar relationships across the mQTL
663 categories (*cis only*, *cis+trans* and *trans only*) (**Figure S45**) though there was insufficient power
664 to quantify selection for *trans only* SNPs. These results can be interpreted that predominantly
665 genetic regions that regulate DNAm are under negative or balancing selection^{60,61} and thus,
666 retain the ancestral DNAm structure. However, a minority of regions containing DNAm sites
667 have experienced positive selection.

668
669 Alleles showing evidence of selection are likely to be biologically meaningful⁶². To investigate
670 whether genetic variants underlying DNAm implicated in selection are linked to diseases/traits,
671 we examined whether GWAS-associated variants from 42 datasets across 11 disease
672 categories were enriched for *cis* mQTL SNPs overlapping extreme SDS scores. After
673 accounting for non-random genomic distribution³⁹, we found that GWAS-associated variants
674 from 19/42 traits were overlapping with at least one *cis* mQTL SNP with extreme SDS. We
675 found an enrichment of mQTL SNPs overlapping extreme SDS scores ($p<2.6e-3$) among
676 variants associated with five traits including extreme height (OR=17.2, $p=1.08e-7$), Crohn's
677 disease (OR=11.3, $p=4.42e-5$), height (OR=1.99, $p=6.76e-5$), schizophrenia (OR=5.28,
678 $p=1.21e-3$) and cardiovascular disease (OR=9.85, $p=1.67e-3$) (**Table S26**). A comparison
679 showed that the genetic variance for cardiovascular disease associated mQTL or height
680 associated mQTL with extreme SDS was higher when compared to all trait associated SNPs
681 suggesting that these loci have been modified by disease pressure (**Figure S46**). To
682 summarize, our results provide the first evidence that selection may have shaped the landscape
683 of DNAm values across the genome and is associated with adaptation on highly polygenic
684 (height) or fitness related (cardiovascular) traits.

685 Implications

686 A map of hundreds of thousands of genetic associations has enabled novel biological insights
687 related to DNAm variation. Using a rigorous analytical framework enabled us to minimise
688 heterogeneity and expand sample sizes for large omic data. This revealed a genetic
689 architecture of DNAm that is polygenic, as with many traits traditionally considered 'complex'.
690 Given the diverse ranges of age, gender proportions and geographical origins between the
691 cohorts in this analysis, the minimal extent of heterogeneity across datasets indicates that
692 genetic effects on DNAm are relatively stable across contexts. We show that *cis* and *trans*
693 mQTL operate through distinct mechanisms, as their genomic properties are distinct. A driver of
694 long-range associations may be co-regulated through TF binding and nuclear organisation.

695
696 Though we found substantial sharing of genetic signals between DNAm sites and complex
697 traits, we were able to demonstrate that this was not predominantly due to DNAm variation
698 being on the causal path from genotype to phenotype. These findings have several implications.
699 First, we anticipate that some previously reported EWAS associations are likely due to reverse
700 causation e.g. the risk factor or genetic liability to disease state itself alters DNAm and not vice
701 versa, or confounding. Second, having found there are strong negative and positive selection
702 pressures acting on mQTL, this may be explained through selection acting on complex traits
703 first. Third, the genetic effects on DNAm that overlap with complex traits likely primarily
704 influence other regulatory factors which in turn influence complex traits and DNAm through
705 diverging pathways. Fourth, if the path from genotype to complex traits is non-linear, for
706 example involving the statistical interactions between different regulatory features¹⁶, then our
707 results indicate that large individual-level multi-omic datasets will be required to dissect such
708 mechanisms.

709
710 The microarray technology used in the majority of cohorts included in this study limited us to
711 analyse only 2% of sites across the genome⁶³, which are biased to promoters and strongly
712 underrepresented regulatory elements. To explore the impact of expanding the coverage of
713 arrays, we calculated the linear relationship between the median number of probes by gene on
714 the 450k array and the median number of *cis* and *trans* mQTL. For each probe, we found an
715 increase of 0.76 *cis* mQTL ($p < 9.03e-16$) and 0.05 *trans* mQTL ($p < 1.47e-05$) in the median
716 (**Figure S47**). A similar increase was seen in non-genic regions. EPIC arrays⁶³ and promising
717 low-cost sequencing technologies⁶⁴ offer an opportunity to make detailed interrogations of
718 enhancer and other regulatory regions, which may be more fruitful in finding causal relationships
719 with complex disease.

720
721 The coverage of the mQTL search in this study was limited by the computational necessity of a
722 multiple stage study design (**Figure S48**). Those mQTL that we discovered with r^2 less than 1%
723 are likely a small fraction of all the mQTL in this category expected to exist (**Figure S49**). Across
724 these DNAm sites, and within the range of mQTL detected in our study ($r^2 > 0.22\%$) we estimate
725 that there are twice as many *cis* mQTL and 22.5 times more *trans* mQTL yet to discover (**Figure**
726 **S49**). This would likely not explain all estimated heritability, indicating that a substantial set of
727 the heritability is due to causal variants with smaller effects than those detectable in our study.
728

729 Overall our data and results have resulted in the most comprehensive atlas of genetic effects to
730 date. We expect that this atlas will be of use to the scientific community for studies of genome
731 regulation and contribute to the development of second generation EWAS.

Figure 1: Discovery and replication of mQTL

a) Study Design. In the first phase, 22 cohorts performed a complete mQTL analysis of up to 480,000 sites against up to 12 million variants; retaining their results for $p < 1e-5$. In the second phase, 120 million SNP-DNAm site pairs selected from the first phase, and GWA catalog SNPs against 345k DNAm sites, were tested in 36 studies (including 20 phase 1 studies) and meta-analysed. **b) Distributions of the weighted mean of DNAm across 36 cohorts for *cis* only, *cis+trans* and *trans* only sites.** Plots are coloured with respect to the genomic annotation. *Cis* only sites showed a bimodal distribution of DNAm. *Cis+trans* sites showed intermediate levels of DNAm. *Trans* only sites showed low levels of DNAm. **c) Discovery and replication effect size estimates** between GoDMC ($n=27,750$) and Generation Scotland ($n=5,101$) for 169,656 mQTL associations. The regression coefficient is 1.13 ($se=0.0007$). **d) Relationship between DNAm site heritability estimates and DNAm variance explained in Generation Scotland.** The regression coefficient for the twin family study was 3.16 ($se=0.008$) and for the twin study 2.91 ($se=0.008$) across 403,353 DNAm sites. The variance explained for DNAm sites with missing r^2 ($n=277,428$) and/or $h^2=0$ (Twin family: $n=80,726$ Twin: 34,537) were set to 0.

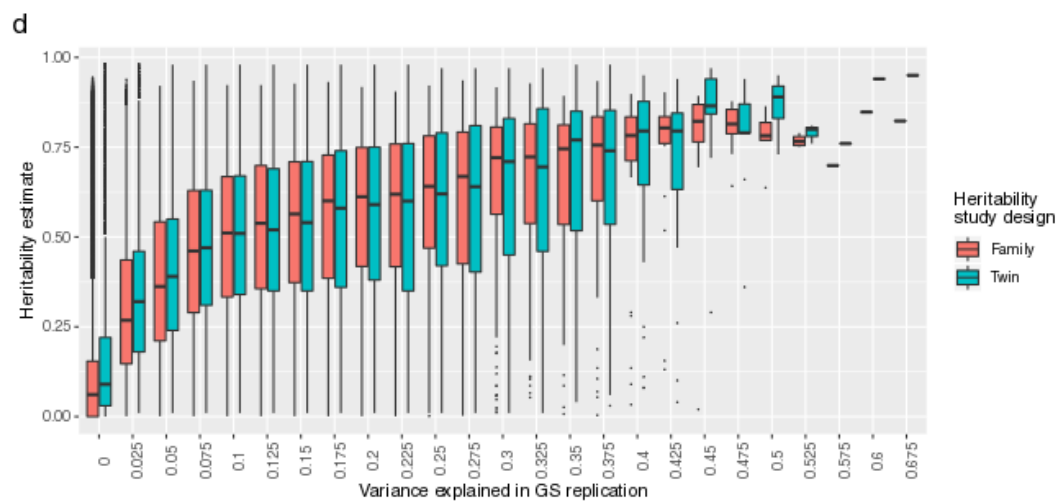
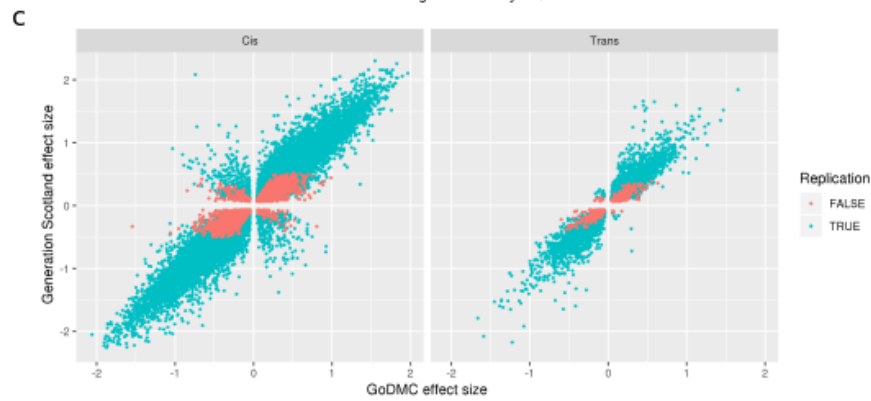
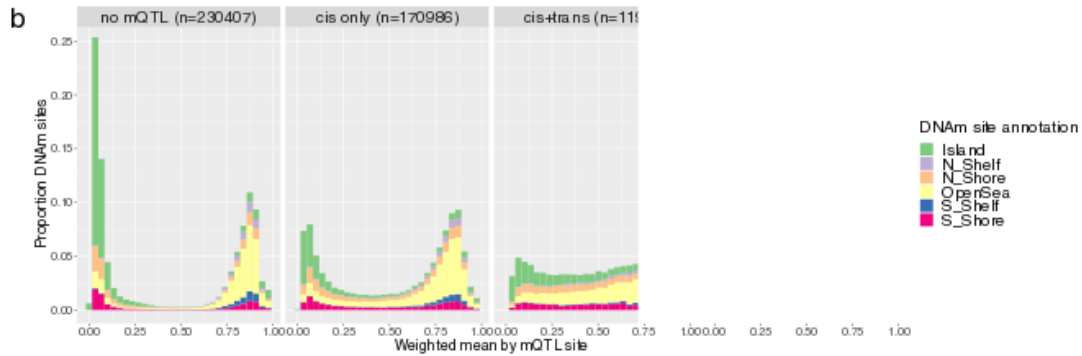
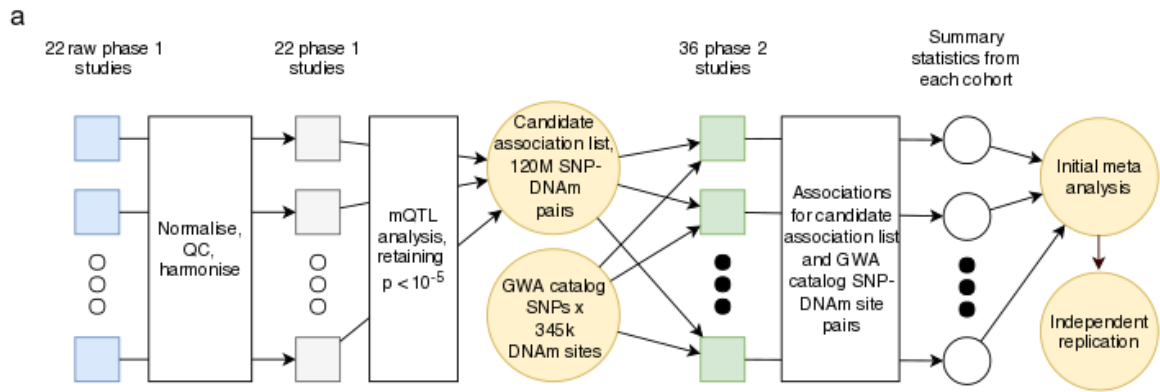


Figure 2: *Cis* and *trans* mQTL operate through distinct mechanisms

Distributions of enrichments for chromatin states and gene annotations among mQTL sites and SNPs. The heatmap represents the distribution of odds ratios for *cis only*, *trans only*, or *cis+trans* sites and SNPs. Significance has been categorised as: *=FDR<0.001; **=FDR<1e-10; ***=FDR<1e-50

b) Distributions of enrichment for occupancy of TFBS among mQTL sites and SNPs. Each density curve represents the distribution of odds ratios for *cis only*, *trans only*, or *cis+trans* sites (left) and SNPs (right).

c) A bipartite graph of the two-dimensional enrichment for *trans*-mQTL. SNPs annotations (blue) with $p_{\text{emp}} < 0.01$ after multiple testing correction co-occur with particular site annotations (red).

d) Distribution of two-dimensional enrichment values of *trans*-mQTL. There was substantial departure from the null in the real dataset for all tissues indicating that the TFBS of a site depended on the TFBS of the SNP that influenced it.

e) Distributions of enrichment of mQTL among 42 complex traits and diseases. Each density curve represents the distribution of odds ratios for *cis only*, *trans only*, or *cis+trans* SNPs.

f) Enrichment of selection signals among mQTL SNPs. Radial lines show odds ratios for the different selection metrics (F_{st} , SDS, iHS, XPEHH (CEU vs CHB) and XPEHH (CEU vs YRI) by site annotation (*cis any*, *cis only*, *cis+trans*, *trans only*, *trans any*). Dots in the inner ring of the outer circle denote enrichment (if present) at thresholds $p < 1e-11$ (outermost) to $p < 1e-14$ (innermost).

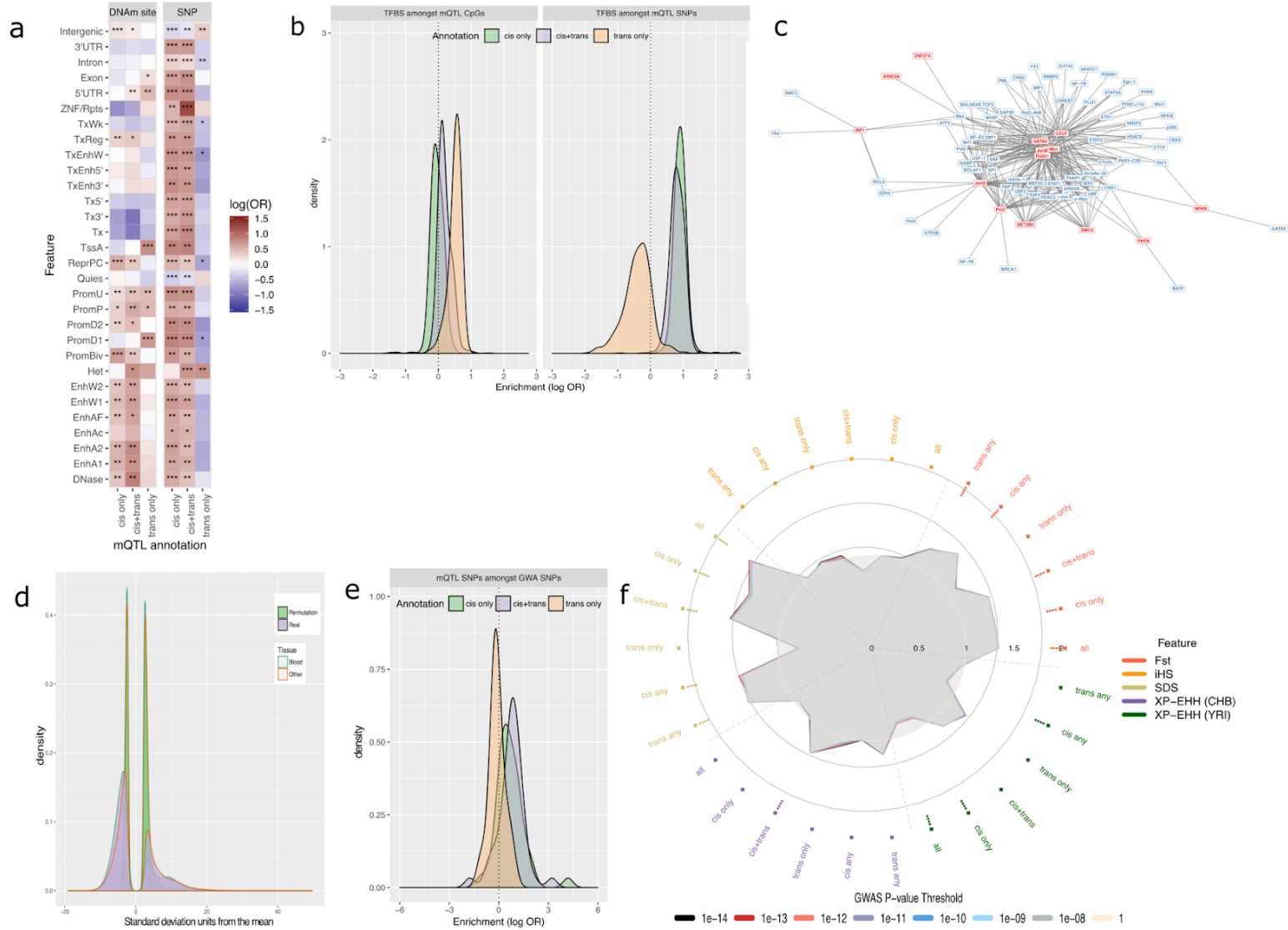


Figure 3: Communities constructed from *trans*-mQTL. **a) A network depicting all communities in which there were twenty or more sites.** Random walks were used to generate communities (colours), so occasionally a DNA site connects different communities. **b) The relationship between genomic annotations, mQTL and communities.** Communities 9 and 22 are comprised of DNAm sites that are related through shared genetic factors. The sankey plots show the genomic annotations for the genetic variants (left) and for the DNAm sites (right). The DNAm sites comprising these communities are enriched for TFBS related to the cohesin complex and NFkB, respectively. **c) Enrichment of GWA traits among community SNPs.** The genomic loci for each of the 56 largest communities were tested for enrichment of low p-values in 133 complex trait GWAS (y-axis). The x-axis depicts the $-\log_{10}$ p-value for enrichment, with the 5% FDR shown by the vertical dotted line. Enrichments were particularly strong for blood related phenotypes (including circulating metal levels).

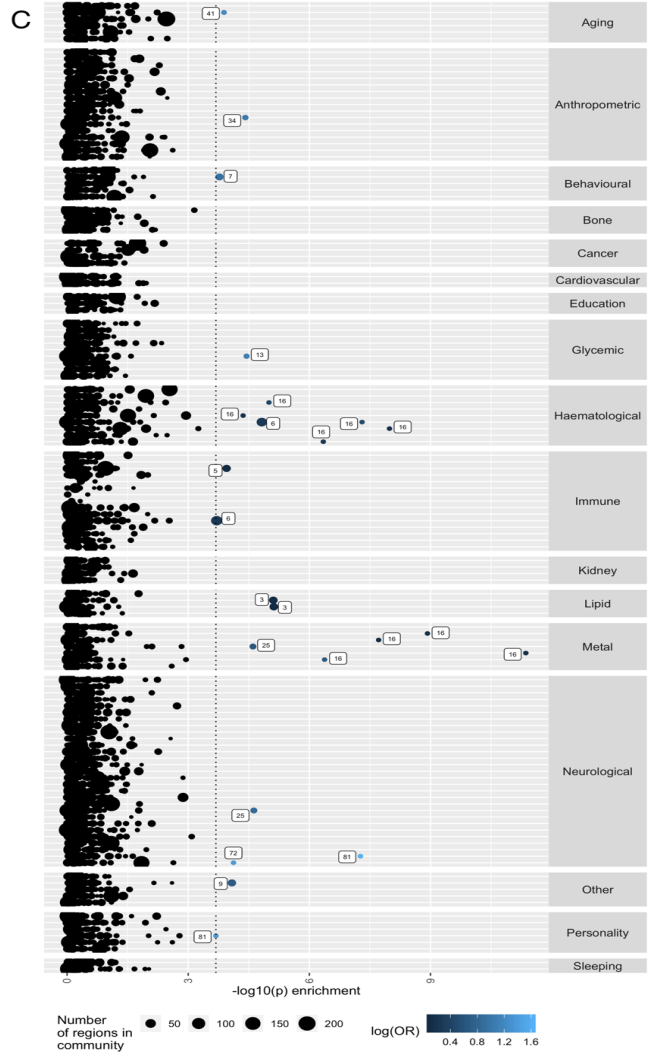
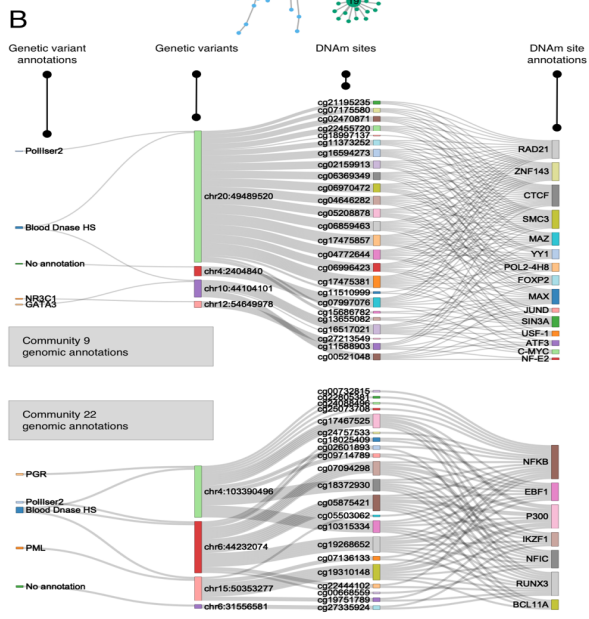
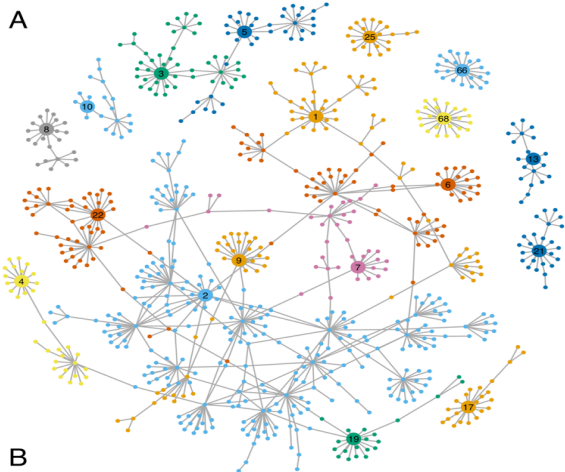
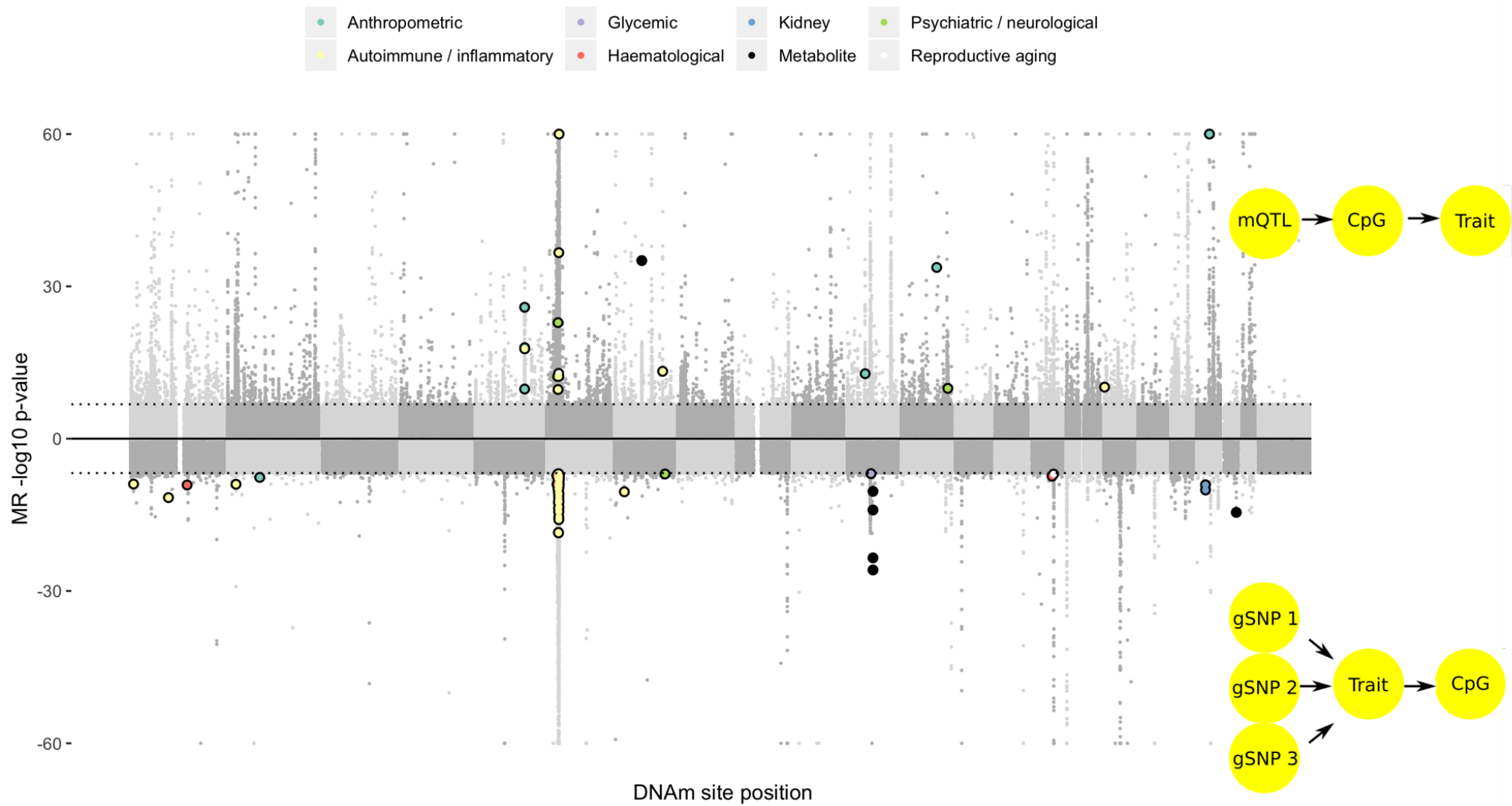


Figure 4: Identifying putative causal relationships between sites and traits using bi-directional MR. Aggregated results from a systematic bi-directional MR analysis between DNAm sites and 116 complex traits. The top plot depicts results from tests of DNAm sites colocalising with complex traits. The light grey points represent MR estimates that either did not surpass multiple testing, or shared small p-values at both the DNAm site and complex trait but had weak evidence of colocalisation. Bold, coloured points are those that showed strong evidence for colocalisation ($H_4 > 0.8$). The bottom plot shows the $-\log_{10}$ p-values from MR analysis of risk factor or genetic liability of disease on DNAm levels. Extensive follow up was performed on DNAm site-trait pairs with putative associations, and those that pass filters are plotted in bold and colored according to the trait category. A substantial number of MR results in both directions exhibited very strong effects but failed to withstand sensitivity analyses



1. Petronis, A. Epigenetics as a unifying principle in the aetiology of complex traits and diseases. *Nature* **465**, 721–727 (2010).
2. McRae, A. F. *et al.* Contribution of genetic variation to transgenerational inheritance of DNA methylation. *Genome Biol.* **15**, R73 (2014).
3. van Dongen, J. *et al.* Genetic and environmental influences interact with age and sex in shaping the human methylome. *Nat. Commun.* **7**, 11115 (2016).
4. Hannon, E. *et al.* Characterizing genetic and environmental influences on variable DNA methylation using monozygotic and dizygotic twins. *PLoS Genet.* **14**, e1007544 (2018).
5. Schadt, E. E. *et al.* Genetics of gene expression surveyed in maize, mouse and man. *Nature* **422**, 297–302 (2003).
6. Davey Smith, G. & Hemani, G. Mendelian randomization: genetic anchors for causal inference in epidemiological studies. *Hum. Mol. Genet.* **23**, R89–R98 (2014).
7. Gaunt, T. R. *et al.* Systematic identification of genetic influences on methylation across the human life course. *Genome Biol.* **17**, 61 (2016).
8. Bonder, M. J. *et al.* Disease variants alter transcription factor levels and methylation of their binding sites. *Nat. Genet.* **49**, 131–138 (2017).
9. Hannon, E. *et al.* Methylation QTLs in the developing brain and their enrichment in schizophrenia risk loci. *Nat. Neurosci.* **19**, 48–54 (2016).
10. Visscher, P. M. *et al.* 10 Years of GWAS Discovery: Biology, Function, and Translation. *Am. J. Hum. Genet.* **101**, 5–22 (2017).
11. 1000 Genomes Project Consortium *et al.* An integrated map of genetic variation from 1,092 human genomes. *Nature* **491**, 56–65 (2012).
12. Yang, J. *et al.* Conditional and joint multiple-SNP analysis of GWAS summary statistics identifies additional variants influencing complex traits. *Nat. Genet.* **44**, 369–75, S1–3 (2012).
13. Lister, R. *et al.* Human DNA methylomes at base resolution show widespread epigenomic differences. *Nature* **462**, 315–322 (2009).

14. Ziller, M. J. *et al.* Charting a dynamic DNA methylation landscape of the human genome. *Nature* **500**, 477–481 (2013).
15. Schübeler, D. Function and information content of DNA methylation. *Nature* **517**, 321–326 (2015).
16. Gutierrez-Arcelus, M. *et al.* Passive and active DNA methylation and the interplay with genetic variation in gene regulation. *Elife* **2**, e00523 (2013).
17. Chen, L. *et al.* Genetic Drivers of Epigenetic and Transcriptional Variation in Human Immune Cells. *Cell* **167**, 1398–1414.e24 (2016).
18. Roadmap Epigenomics Consortium *et al.* Integrative analysis of 111 reference human epigenomes. *Nature* **518**, 317–330 (2015).
19. McRae, A. F. *et al.* Identification of 55,000 Replicated DNA Methylation QTL. *Sci. Rep.* **8**, 17605 (2018).
20. Wahl, S. *et al.* Epigenome-wide association study of body mass index, and the adverse outcomes of adiposity. *Nature* **541**, 81–86 (2017).
21. Elliott, G. *et al.* Intermediate DNA methylation is a conserved signature of genome regulation. *Nat. Commun.* **6**, 6363 (2015).
22. Grundberg, E. *et al.* Global analysis of DNA methylation variation in adipose tissue from twins reveals links to disease-associated variants in distal regulatory elements. *Am. J. Hum. Genet.* **93**, 876–890 (2013).
23. Qi, T. *et al.* Identifying gene targets for brain-related traits using transcriptomic and methylomic data from blood. *Nat. Commun.* **9**, 2282 (2018).
24. Feldmann, A. *et al.* Transcription factor occupancy can mediate active turnover of DNA methylation at regulatory regions. *PLoS Genet.* **9**, e1003994 (2013).
25. Stadler, M. B. *et al.* DNA-binding factors shape the mouse methylome at distal regulatory regions. *Nature* **480**, 490–495 (2011).
26. ENCODE Project Consortium. An integrated encyclopedia of DNA elements in the human genome. *Nature* **489**, 57–74 (2012).
27. Sánchez-Castillo, M. *et al.* CODEX: a next-generation sequencing experiment database for

- the haematopoietic and embryonic stem cell communities. *Nucleic Acids Res.* **43**, D1117–23 (2015).
28. Viny, A. D. *et al.* Dose-dependent role of the cohesin complex in normal and malignant hematopoiesis. *J. Exp. Med.* **212**, 1819–1832 (2015).
 29. GTEx Consortium *et al.* Genetic effects on gene expression across human tissues. *Nature* **550**, 204–213 (2017).
 30. Chinenov, Y., Coppo, M., Gupte, R., Sacta, M. A. & Rogatsky, I. Glucocorticoid receptor coordinates transcription factor-dominated regulatory network in macrophages. *BMC Genomics* **15**, 656 (2014).
 31. Geller, D. A. *et al.* Cytokine induction of interferon regulatory factor-1 in hepatocytes. *Surgery* **114**, 235–242 (1993).
 32. Gilchrist, M. *et al.* Systems biology approaches identify ATF3 as a negative regulator of Toll-like receptor 4. *Nature* **441**, 173–178 (2006).
 33. Yang, J., Tian, B., Sun, H., Garofalo, R. P. & Brasier, A. R. Epigenetic silencing of IRF1 dysregulates type III interferon responses to respiratory virus infection in epithelial to mesenchymal transition. *Nat Microbiol* **2**, 17086 (2017).
 34. Rao, S. S. P. *et al.* A 3D map of the human genome at kilobase resolution reveals principles of chromatin looping. *Cell* **159**, 1665–1680 (2014).
 35. Astle, W. J. *et al.* The Allelic Landscape of Human Blood Cell Trait Variation and Links to Common Complex Disease. *Cell* **167**, 1415–1429.e19 (2016).
 36. Maurano, M. T. *et al.* Systematic localization of common disease-associated variation in regulatory DNA. *Science* **337**, 1190–1195 (2012).
 37. Tachmazidou, I. *et al.* Whole-Genome Sequencing Coupled to Imputation Discovers Genetic Signals for Anthropometric Traits. *Am. J. Hum. Genet.* **100**, 865–884 (2017).
 38. Kato, N. *et al.* Trans-ancestry genome-wide association study identifies 12 genetic loci influencing blood pressure and implicates a role for DNA methylation. *Nat. Genet.* **47**, 1282–1293 (2015).
 39. Iotchkova, V. *et al.* GARFIELD classifies disease-relevant genomic features through

- integration of functional annotations with association signals. *Nat. Genet.* **51**, 343–353 (2019).
40. Schork, A. J. *et al.* All SNPs are not created equal: genome-wide association studies reveal a consistent pattern of enrichment among functionally annotated SNPs. *PLoS Genet.* **9**, e1003449 (2013).
 41. Houseman, E. A. *et al.* DNA methylation arrays as surrogate measures of cell mixture distribution. *BMC Bioinformatics* **13**, 86 (2012).
 42. Reinius, L. E. *et al.* Differential DNA methylation in purified human blood cells: implications for cell lineage and studies on disease susceptibility. *PLoS One* **7**, e41361 (2012).
 43. Hemani, G., Tilling, K. & Davey Smith, G. Orienting the causal relationship between imprecisely measured traits using GWAS summary data. *PLoS Genet.* **13**, e1007081 (2017).
 44. Giambartolomei, C. *et al.* Bayesian test for colocalisation between pairs of genetic association studies using summary statistics. *PLoS Genet.* **10**, e1004383 (2014).
 45. Zhu, Z. *et al.* Integration of summary data from GWAS and eQTL studies predicts complex trait gene targets. *Nat. Genet.* **48**, 481–487 (2016).
 46. Zheng, J. *et al.* Phenome-wide Mendelian randomization mapping the influence of the plasma proteome on complex diseases. *bioRxiv* 627398 (2019) doi:10.1101/627398.
 47. Richardson, T. G. *et al.* Systematic Mendelian randomization framework elucidates hundreds of CpG sites which may mediate the influence of genetic variants on disease. *Hum. Mol. Genet.* (2018) doi:10.1093/hmg/ddy210.
 48. Hemani, G., Bowden, J. & Davey Smith, G. Evaluating the potential role of pleiotropy in Mendelian randomization studies. *Hum. Mol. Genet.* **27**, R195–R208 (2018).
 49. Kilpinen, H. *et al.* Coordinated effects of sequence variation on DNA binding, chromatin structure, and transcription. *Science* **342**, 744–747 (2013).
 50. Banovich, N. E. *et al.* Methylation QTLs are associated with coordinated changes in transcription factor binding, histone modifications, and gene expression levels. *PLoS Genet.* **10**, e1004663 (2014).

51. Brion, M.-J. a., Shakhbazov, K. & Visscher, P. M. Calculating statistical power in Mendelian randomization studies. *Int. J. Epidemiol.* **42**, 1497–1501 (2013).
52. Pierce, B. L. & Burgess, S. Efficient design for Mendelian randomization studies: subsample and 2-sample instrumental variable estimators. *Am. J. Epidemiol.* **178**, 1177–1184 (2013).
53. Hemani, G. *et al.* The MR-Base platform supports systematic causal inference across the human phenome. *Elife* **7**, (2018).
54. Dekkers, K. F. *et al.* Blood lipids influence DNA methylation in circulating cells. *Genome Biol.* **17**, 138 (2016).
55. Braun, K. V. E. *et al.* Epigenome-wide association study (EWAS) on lipids: the Rotterdam Study. *Clin. Epigenetics* **9**, 15 (2017).
56. Byars, S. G. *et al.* Genetic loci associated with coronary artery disease harbor evidence of selection and antagonistic pleiotropy. *PLoS Genet.* **13**, e1006328 (2017).
57. Turchin, M. C. *et al.* Evidence of widespread selection on standing variation in Europe at height-associated SNPs. *Nat. Genet.* **44**, 1015–1019 (2012).
58. Field, Y. *et al.* Detection of human adaptation during the past 2000 years. *Science* **354**, 760–764 (2016).
59. Zeng, J. *et al.* Widespread signatures of negative selection in the genetic architecture of human complex traits. (2017) doi:10.1101/145755.
60. Johnson, T. & Barton, N. Theoretical models of selection and mutation on quantitative traits. *Philos. Trans. R. Soc. Lond. B Biol. Sci.* **360**, 1411–1425 (2005).
61. Eyre-Walker, A. Evolution in health and medicine Sackler colloquium: Genetic architecture of a complex trait and its implications for fitness and genome-wide association studies. *Proc. Natl. Acad. Sci. U. S. A.* **107 Suppl 1**, 1752–1756 (2010).
62. Vitti, J. J., Grossman, S. R. & Sabeti, P. C. Detecting natural selection in genomic data. *Annu. Rev. Genet.* **47**, 97–120 (2013).
63. Pidsley, R. *et al.* Critical evaluation of the Illumina MethylationEPIC BeadChip microarray for whole-genome DNA methylation profiling. *Genome Biol.* **17**, 208 (2016).

64. Simpson, J. T. *et al.* Detecting DNA cytosine methylation using nanopore sequencing. *Nat. Methods* **14**, 407–410 (2017).